Paper AAS 99-317

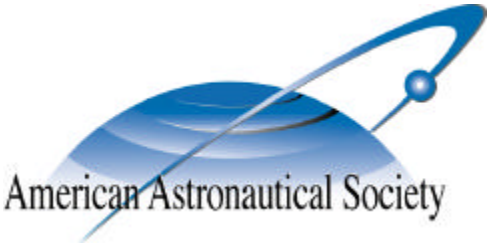

Satellite Attitude Control and Power Tracking with Momentum Wheels

Panagiotis Tsiotras and Haijun Shen
Georgia Institute of Technology
Atlanta, GA 30332-0150, USA

Chris Hall
Virginia Polyutechnic Institute and State University
Blacksburg, VA 24061-0203, USA

AAS/AIAA Astrodynamics Specialist Conference

Girdwood, Alaska 16-19 August 1999

AAS Publications Office, P.O. Box 28130, San Diego, CA 92129

Satellite Attitude Control and Power Tracking with Momentum Wheels

Panagiotis Tsiotras* and Haijun Shen†
Georgia Institute of Technology
Atlanta, GA 30332-0150, USA

Chris Hall‡
Virginia Polytechnic Institute and State University
Blacksburg, VA 24061-0203, USA

A control law for an Integrated Power/Attitude Control System (IPACS) for a satellite is presented in this paper. Four non-coplanar momentum wheels in a special configuration, and a set of three thrusters are used to implement the torque inputs. The momentum wheels are used as attitude control actuators, as well as an energy storage mechanism, providing power to the spacecraft. In that respect, they can be used to replace the currently used heavy chemical batteries. The thrusters are used to implement large torques for large and fast (slew) maneuvers and provide for the momentum management strategies. The momentum wheels are used to provide the reference-tracking torques and the torques for speeding up or slowing down the wheels for storing and releasing kinetic energy. The attitude tracking controller published in a previous work is adopted here. Power tracking for charging and discharging the momentum wheels is added to complete the IPACS framework. The torques applied by the momentum wheels are decomposed into two spaces which are perpendicular to each other, with the attitude control torques and power tracking torques in each space. This control law can be easily incorporated in an IPACS system on-board a satellite. The possibility of occurrence of singularities, where no arbitrary energy profile can be tracked, is studied for the wheel cluster considered in the paper. A generic momentum management scheme is considered to null the total angular momentum of the wheels so as to minimize the gyroscopic effects and prevent the singularity from occurring. A numerical example for a low earth near polar orbital satellite is provided to test the proposed IPACS algorithm. The satellite's boresight axis is required to track a ground station. In addition, the satellite is required to rotate about its boresight axis so that the solar panel axis is perpendicular to the satellite-sun vector.

Introduction

The Integrated Power and Attitude Control System (IPACS) concept has been studied since the 1960s, but has been particularly popular during the 1980s. Most spacecraft use chemical batteries (NiCd, NiH_2, usually) to store excess energy generated by the solar panels during periods of exposure to the sun.[1] During eclipse, the batteries are used to provide power for the spacecraft subsystems. The batteries are recharged when the spacecraft exits the eclipse. The primary problem with this approach is the cycle life of batteries and the additional power system mass required to control the charging and discharging cycles.

The use of flywheels instead of batteries to store energy on spacecraft was suggested as early as 1961 in the article by Roes,[2] when a 17 Whr/kg composite flywheel spinning at 10,000 to 20,000 rpm on magnetic bearings was proposed. The configuration included two counter-rotating flywheels, and the author did not mention the possibility of using the momentum for attitude control. However, since many spacecraft use flywheels (momentum wheels, control moment gyros, etc.) to control attitude, the integration of these two functions is naturally of interest. Numerous studies of this integration have been conducted. For instance, Adams[3] investigated the use of a particular class of flywheels made of flexible filaments, focusing on energy and momentum storage capabilities. Anderson and Keckler[4] originated the term "IPACS" in 1973. A study by Cormack[5] done for Rockwell examined the use of an integrated IPACS system. Keckler and Jacobs[6] presented a description of the concept. Will *et al.*[7] investigated the IPACS concept and performed simulations using the (linearized) equations of motion. Notti *et al.*[8] performed an extensive systems study and investigated linear control laws for attitude control. Their study included trade studies on the use of momentum wheels, control moment gyros, and counter-rotating pairs. NASA and Boeing also conducted separate studies on the IPACS concept.[9,10] Gross[10] summarized his findings in a workshop presentation.[11] Anand *et al.*[12,13] discussed the system design issues associated with using magnetic bearings, as did Downer *et al.*[14] Flatley[15] studied a tetrahedron array of four momentum wheels, and considered the issues associated with simultaneously torquing the wheels for attitude control and energy storage. Around

*Associate Professor, School of Aerospace Engineering, Georgia Institute of Technology. Email: p.tsiotras@ae.gatech.edu. Senior member AIAA.

†Graduate Student, School of Aerospace Engineering, Georgia Institute of Technology. Email: gt7318d@prism.gatech.edu. Student member AIAA.

‡Associate Professor, Department of Aerospace and Ocean Engineering, Virginia Polytechnic Institute and State University, Email: chall@aoe.vt.edu. Associate Fellow AIAA,

the same time with Flatley's work, O'dea *et al.*[16] included simultaneous attitude determination in their study of a combined Attitude, Reference, and Energy Storage (CARES) system, focusing on technology-related issues. Oglevie and Eisenhaure[17,18] performed a system level study of IPACS systems, and Ref. 17 included a substantial list of references to earlier work. Olmsted[19] presented the technology-related issues associated with a particular flywheel design. Optimal design criteria associated with an integrated Attitude Control and Energy Storage (ACES) system were discussed by Studer and Rodriguez.[20] The articles by Van Tassel and Simon[21] and Olszewski[22,23] described the key technologies involved in IPACS. Finally, Rockwell conducted a system study for NASA (Santo *et al.*[24]), focusing on space station applications.

Most of these previous investigations of IPACS focus on general design issues. The exact nonlinear equations of motions are not considered even when the attitude control results are provided. In this paper, the exact nonlinear equations of motion are used to design an attitude controller which tracks a reference attitude profile. The momentum wheel control torque space is decomposed into two spaces which are perpendicular to each other. The attitude control torques lie in one of these two spaces, and the torques in the other space are used to speed up or slow down the momentum wheels to store or extract kinetic energy. In the following, the system model is given first, then the reference attitude and momentum wheel power tracking controllers are presented. A numerical example considering a IRIDIUM-type satellite in orbit is provided to illustrate the proposed IPACS methodology.

System model

Dynamics

Consider a rigid spacecraft with an N-momentum-wheel cluster installed to provide internal torques. Let $\mathbf{B}$ denote the spacecraft body frame. Then the rotational equations of motion for the spacecraft can be expressed as

$$\dot{\mathbf{h}}_B = \mathbf{h}_B^{\times}\mathbf{J}^{-1}(\mathbf{h}_B - \mathbf{A}\mathbf{h}_a) + \mathbf{g}_e \tag{1a}$$

$$\dot{\mathbf{h}}_a = \mathbf{g}_a \tag{1b}$$

where $\mathbf{h}_B$ is the angular momentum vector of the spacecraft in the $\mathbf{B}$ frame, given by

$$\mathbf{h}_B = \mathbf{J}\boldsymbol{\omega}_B + \mathbf{A}\mathbf{h}_a \tag{2}$$

where $\mathbf{h}_a$ is the $N \times 1$ vector of the *axial* angular momenta of the wheels, $\boldsymbol{\omega}_B$ is the angular velocity vector of the spacecraft in the $\mathbf{B}$ frame, $\mathbf{g}_e$ is the 3×1 vector of external torques, $\mathbf{g}_a$ is the $N \times 1$ vector of the internal axial torques applied by the platform to the momentum wheels, and $\mathbf{A}$ is the $3 \times N$ matrix whose columns contain the axial unit vectors of the N momentum wheels. $\mathbf{J}$ is an inertia-like matrix defined as

$$\mathbf{J} = \mathbf{I} - \mathbf{A}\mathbf{I}_s\mathbf{A}^T \tag{3}$$

where $\mathbf{I}$ is the moment of inertia of the spacecraft, including the momentum wheels.

The *axial* angular momentum vector of the momentum wheels can be written as

$$\mathbf{h}_a = \mathbf{I}_s\mathbf{A}^T\boldsymbol{\omega}_B + \mathbf{I}_s\boldsymbol{\omega}_s \tag{4}$$

where $\boldsymbol{\omega}_s = (\omega_{s1}, \omega_{s2}, \ldots, \omega_{sN})^T$ is an $N \times 1$ vector denoting the axial angular velocity of the momentum wheels with respect to the spacecraft. We will later denote the total axial angular velocity of the momentum wheels relative to the inertial frame as $\boldsymbol{\omega}_c = (\omega_{c1}, \omega_{c2}, \ldots, \omega_{cN})^T$. Using this notation, the following is true,

$$\mathbf{h}_a = \mathbf{I}_s\mathbf{A}^T\boldsymbol{\omega}_B + \mathbf{I}_s\boldsymbol{\omega}_s = \mathbf{I}_s\boldsymbol{\omega}_c \tag{5}$$

that is, $\boldsymbol{\omega}_c = \boldsymbol{\omega}_s + \mathbf{A}^T\boldsymbol{\omega}_B$. Notice that since typically the wheels spin at a much higher speed than the spacecraft itself, $\boldsymbol{\omega}_s >> \boldsymbol{\omega}_B$ and we have that $\boldsymbol{\omega}_c \approx \boldsymbol{\omega}_c$.

Kinematics

The so-called "Modified Rodrigues Parameters" (MRPs) given in Refs. 25–27 will be chosen to describe the error attitude kinematics of the spacecraft. The MRPs are defined in terms of the Euler principal vector, $\mathbf{e}$, and angle ϕ, by

$$\boldsymbol{\sigma}_B = \mathbf{e}\tan(\phi/4) \tag{6}$$

The MRPs have the advantage of being well-defined for the whole range for rotations, i.e., $\phi \in [0, 2\pi)$. The differential equation governing the kinematics in terms of MRPs is given by

$$\dot{\boldsymbol{\sigma}}_B = \mathbf{G}(\boldsymbol{\sigma}_B)\boldsymbol{\omega}_B \tag{7}$$

where

$$\mathbf{G}(\boldsymbol{\sigma}_B) = \frac{1}{2}\left(\mathbf{1} + \boldsymbol{\sigma}_B^{\times} + \boldsymbol{\sigma}_B\boldsymbol{\sigma}_B^T - \frac{1+\boldsymbol{\sigma}_B^T\boldsymbol{\sigma}_B}{2}\mathbf{1}\right) \tag{8}$$

and $\mathbf{1}$ is the 3×3 identity matrix.

Tracking controller

In the previous work by the authors,[28] three control laws were presented to track a reference attitude profile. Here we restate the controller II of Ref. 28, which assumes that the reference frame dynamics and kinematics are given by

$$\dot{\mathbf{h}}_R = \mathbf{h}_R^{\times}\mathbf{J}^{-1}\mathbf{h}_R + \mathbf{g}_R \tag{9}$$

$$\dot{\boldsymbol{\sigma}}_R = \mathbf{G}(\boldsymbol{\sigma}_R)\boldsymbol{\omega}_R \tag{10}$$

where the subscript R stands for the reference frame to be tracked.

The external torques are assumed to include the torque due to thruster firing, the gravity gradient torque and the other disturbance torques; i.e.,

$$\mathbf{g}_e = \mathbf{g}_t + \mathbf{g}_g + \mathbf{g}_d \tag{11}$$

where the subscripts t, g, and d denote the thruster, gradient, and disturbance, respectively. The gravity gradient torque is given by[29]

$$\mathbf{g}_g = \frac{3\mu}{R_c^3}\mathbf{c}_3^{\times}\mathbf{I}\mathbf{c}_3 \tag{12}$$

where $\mathbf{r}_c$ is the vector from the earth center to the spacecraft center of mass with $R_c = |\mathbf{r}_c|$, $\mathbf{c}_3$ is a vector consisting of the three components of the unit vector $-\mathbf{r}_c/R_c$ in the body frame, and $\mu = 3.986005 \times 10^5 \mathrm{km}^3\mathrm{s}^{-2}$ is a constant.

Define the angular velocity tracking error in the body frame as

$$\delta\boldsymbol{\omega} = \boldsymbol{\omega}_B - \mathbf{C}_R^B(\delta\boldsymbol{\sigma})\boldsymbol{\omega}_R \tag{13}$$

with $\mathbf{C}_R^B(\delta\boldsymbol{\sigma})$ being the rotation matrix from the reference frame $\mathbf{R}$ to the body frame $\mathbf{B}$, and $\delta\boldsymbol{\sigma}$ being the MRPs between the reference frame and the body frame; i.e.,

$$\mathbf{C}_R^B(\delta\boldsymbol{\sigma}) = \mathbf{C}_N^B(\boldsymbol{\sigma}_B)[\mathbf{C}_N^B(\boldsymbol{\sigma}_R)]^T \tag{14}$$

and the kinematics error satisfies the following differential equation

$$\delta\dot{\boldsymbol{\sigma}} = \mathbf{G}(\delta\boldsymbol{\sigma})\delta\boldsymbol{\omega} \tag{15}$$

The control law is found by the following Lyapunov function

$$V = \frac{1}{2}\delta\boldsymbol{\omega}^T\mathbf{K}\delta\boldsymbol{\omega} + 2k_2\ln(1+\delta\boldsymbol{\sigma}^T\delta\boldsymbol{\sigma}) \tag{16}$$

where $\mathbf{K} = \mathbf{K}^T > 0$, and $k_2 > 0$. This function is positive definite and radially unbounded[30] in terms of the tracking errors $\delta\boldsymbol{\omega}$ and $\delta\boldsymbol{\sigma}$. Taking the derivative of V and using Eqs. (13) and (15) yields the time derivative of V in terms of $\boldsymbol{\omega}_B$, $\boldsymbol{\omega}_R$ and the tracking error $\delta\boldsymbol{\omega}$ and $\delta\boldsymbol{\sigma}$, i.e.,

$$\begin{aligned}\dot{V} =& \delta\boldsymbol{\omega}^T\left[\mathbf{h}_B^{\times}\mathbf{J}^{-1}(\mathbf{h}_B - \mathbf{A}\mathbf{h}_a) + \mathbf{g}_e - \mathbf{J}\boldsymbol{\omega}_B^{\times}\delta\boldsymbol{\omega}\right.\\ &-\mathbf{J}\mathbf{C}_R^B(\delta\boldsymbol{\sigma})\mathbf{J}^{-1}\mathbf{h}_R^{\times}\mathbf{J}^{-1}\mathbf{h}_R - \mathbf{J}\mathbf{C}_R^B(\delta\boldsymbol{\sigma})\mathbf{J}^{-1}\mathbf{g}_R\\ &\left.-\mathbf{A}\mathbf{g}_a + k_2\delta\boldsymbol{\sigma}\right]\end{aligned} \tag{17}$$

where $\mathbf{K}$ is chosen to be $\mathbf{J}^{-1}$. Then the controllers $\mathbf{g}_t$ and $\mathbf{A}\mathbf{g}_a = \mathbf{f}$ are chosen such that

$$\dot{V} = -k_1\delta\boldsymbol{\omega}^T\delta\boldsymbol{\omega} \leq 0 \tag{18}$$

where $k_1 > 0$. As shown in Ref. 28, the tracking error system is asymptotically stable; i.e., $\boldsymbol{\omega}_B \to \boldsymbol{\omega}_R$, and $\boldsymbol{\sigma}_B \to \boldsymbol{\sigma}_R$ as $t \to \infty$.

A potential difficulty with this approach is that the control inputs are actually the internal torques $\mathbf{g}_a$ which have to be solved from $\mathbf{A}\mathbf{g}_a = \mathbf{f}$. If $N < 3$, the system is overdetermined and a solution may not exist; if $N = 3$, (and for non-coplanar momentum wheels), the solution is uniquely determined; and if $N > 3$, the system is underdetermined and there exists an infinite number of solutions. In particular, in the latter case every solution has the form $\mathbf{g}_a = \mathbf{g}_r + \mathbf{g}_n$, where $\mathbf{g}_r$ belongs to the range space $R(\mathbf{A}^T)$ of the matrix $\mathbf{A}^T$ and $\mathbf{g}_n$ belongs to the null space $N(\mathbf{A})$ of the matrix $\mathbf{A}$.

It is seen that $\mathbf{g}_n$ does not contribute to the attitude control input since $\mathbf{A}\mathbf{g}_n = 0$. One can always choose the torque $\mathbf{g}_r$ to fulfill $\mathbf{A}\mathbf{g}_r = \mathbf{f}$, and subsequently use $\mathbf{g}_n$ to perform power/energy storage management.[31] Notice that this approach can be implemented as long as $N(\mathbf{A})$ has nonzero basis, which is always true for a cluster with more than three non-coplanar momentum wheels.

In the following section, we will consider a four momentum-wheel cluster and construct the torques in the null space of $\mathbf{A}$, so as not to disturb the attitude control operation of the spacecraft, and to track a desired power profile. In other words, the power and attitude tracking operations are performed simultaneously and independent of one another. Power tracking objectives do not interfere with attitude tracking objectives and vice versa. We insist on this separation of objectives since it is unlikely that any IPACS system which compromises either power or attitude control requirement will be acceptable for use in routine spacecraft operations.

Power tracking

As shown in the previous section, the torque required to control the motion is given by an expression of the form

$$\mathbf{A}\mathbf{g}_a = \mathbf{f} \tag{19}$$

where $\mathbf{f}$ is the 3×1 required torque vector. The general solution for $\mathbf{g}_a$ is given by

$$\mathbf{g}_a = \mathbf{A}^{+}\mathbf{f} + \mathbf{g}_n \tag{20}$$

where $\mathbf{A}^{+} = \mathbf{A}^T(\mathbf{A}\mathbf{A}^T)^{-1}$ is the projection operator on the range of $\mathbf{A}^T$, and thus $\mathbf{A}^{+}\mathbf{f} = \mathbf{g}_r \in R(\mathbf{A}^T)$, and where $\mathbf{g}_n \in N(\mathbf{A})$; i.e.,

$$\mathbf{A}\mathbf{g}_n = 0 \tag{21}$$

Note that $\mathbf{A}\mathbf{g}_a = \mathbf{A}(\mathbf{A}^{+}\mathbf{f} + \mathbf{g}_n) = \mathbf{f}$, so $\mathbf{g}_n$ does not affect the spacecraft motion.

The total kinetic energy stored in the momentum wheels is

$$T = \frac{1}{2}\boldsymbol{\omega}_c^T\mathbf{I}_s\boldsymbol{\omega}_c \tag{22}$$

The power (rate of change of the energy), is given by

$$\frac{\mathrm{d}T}{\mathrm{d}t} = P = \boldsymbol{\omega}_c^T\mathbf{I}_s\dot{\boldsymbol{\omega}}_c \tag{23}$$

The objective here is to find a controller $\mathbf{g}_n$ in the null space of $\mathbf{A}$ to provide the required power function $P(t)$. Equation (5) implies that $\mathbf{g}_a = \dot{\mathbf{h}}_a = \mathbf{I}_s\dot{\boldsymbol{\omega}}_c$, so from Eq. (23) we have

$$\boldsymbol{\omega}_c^T\mathbf{g}_a = P \tag{24}$$

Therefore, simultaneous attitude control and power management requires a control torque vector $\mathbf{g}_a$ satisfying the following set of linear equations

$$\begin{bmatrix} \mathbf{A} \\ \boldsymbol{\omega}_c^T \end{bmatrix} \mathbf{g}_a = \begin{bmatrix} \mathbf{f} \\ P \end{bmatrix} \tag{25}$$

From Eq. (20), we have that the torque $\mathbf{g}_n$ in the null space of $\mathbf{A}$ has to satisfy

$$\boldsymbol{\omega}_c^T (\mathbf{A}^+ \mathbf{f} + \mathbf{g}_n) = P \tag{26}$$

or letting $P_m = P - \boldsymbol{\omega}_c^T \mathbf{A}^+ \mathbf{f}$,

$$\boldsymbol{\omega}_c^T \mathbf{g}_n = P_m \tag{27}$$

Since $\mathbf{g}_n \in N(A)$, there always exists a vector $\nu \in \mathbb{R}^N$ such that

$$\mathbf{g}_n = P_N \nu \tag{28}$$

where $P_N = \mathbf{1}_N - \mathbf{A}^T (\mathbf{A}\mathbf{A}^T)^{-1}\mathbf{A}$ is the (orthogonal) projection on $N(A)$. Thus, we have $\boldsymbol{\omega}_c^T P_N \nu = P_m$, to which a minimum norm solution is given by

$$\nu = P_N \boldsymbol{\omega}_c (\boldsymbol{\omega}_c^T P_N \boldsymbol{\omega}_c)^{-1} P_m \tag{29}$$

and the energy management torque $\mathbf{g}_n$ can then be chosen as

$$\mathbf{g}_n = P_N \boldsymbol{\omega}_c (\boldsymbol{\omega}_c^T P_N \boldsymbol{\omega}_c)^{-1} P_m \tag{30}$$

A solution of Eq. (30) exists, as long as $P_N \boldsymbol{\omega}_c \neq 0$. This implies, that either $\boldsymbol{\omega}_c \neq 0$ or $\boldsymbol{\omega}_c \notin N(\mathbf{A})^\perp = R(\mathbf{A}^T)$. The last requirement is also evident from Eq. (25), where the matrix in the left hand side does not have full row rank if $\boldsymbol{\omega}_c \in R(\mathbf{A}^T)$.

It should be pointed out that for satellite applications, during sunlight the solar panels provide enough power for the spacecraft equipment, and the wheels spin up to absorb and store the excess energy. Moreover, typically the sunlight period is longer than the eclipse period. Therefore, the significance of tracking a specific power function is less during the sunlight than during the eclipse period when the power is solely provided by spinning down the momentum wheels. Some authors have therefore chosen to discard power tracking altogether and simply spin up the wheels during sunlight to store the excess energy. This is the approach used, for example, in Ref.[15] On the contrary, unloading of the wheels during the eclipse is more critical, since the wheel deceleration should be done at a certain *rate* in order to provide the necessary power to the spacecraft bus.

Singularity Avoidance and Momentum Management

So far, we have found a controller $\mathbf{g}_a$ which tracks desired power profiles, while controlling the spacecraft attitude. In addition, as was mentioned already, from Eq. (27) we can see that if $\boldsymbol{\omega}_c$ lies in the range space of $\mathbf{A}^T$, then since $\mathbf{g}_n$ is in the null space of $\mathbf{A}$, we have

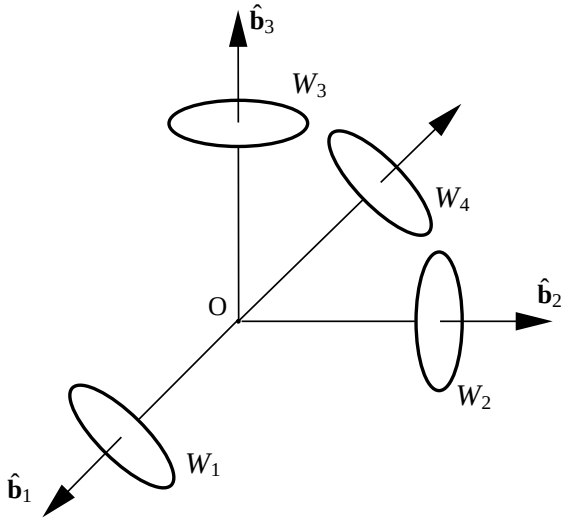

Fig. 1 The configuration of momentum wheels.

$$\boldsymbol{\omega}_c^T \mathbf{g}_n = 0 \tag{31}$$

This implies that the controller loses the capability of tracking an arbitrary power function, and from Eq. (26) the only power the wheels can supply is $\boldsymbol{\omega}_c^T \mathbf{A}^+ \mathbf{f}$. However, the latter case is undesirable in many practical applications. For example, for a stabilized spacecraft when the torque $\mathbf{f}$ is small, the amount of supplied power can be less than the required power level during the singularity.

To take a closer look at the singularity problem, and how it can be avoided by proper momentum management, we consider the four momentum-wheel cluster shown in Fig. 1. The wheels are assumed to have the same axial moment of inertia which is denoted by I_s. The $\mathbf{A}$ matrix in this case is given by

$$\mathbf{A} = \begin{bmatrix} 1 & 0 & 0 & \frac{\sqrt{3}}{3} \\ 0 & 1 & 0 & \frac{\sqrt{3}}{3} \\ 0 & 0 & 1 & \frac{\sqrt{3}}{3} \end{bmatrix} \tag{32}$$

Thus, the case when $\boldsymbol{\omega}_c$ is in the range space of $\mathbf{A}^T$ implies that

$$\omega_{c4} = \frac{\sqrt{3}}{3}(\omega_{c1} + \omega_{c2} + \omega_{c3}). \tag{33}$$

which further implies (since $h_{ai} = I_{si}\omega_{ci}, i = 1, \ldots, 4$) that in the case of singularity the angular momentum of the wheels satisfies the equation

$$h_{a4} = \frac{\sqrt{3}}{3} \sum_{i=1}^{3} h_{ai}. \tag{34}$$

If the angular momenta of the momentum wheels are not distributed such that the total angular momentum of

the wheels stay close to zero, the gyroscopic torques will play a significant role, increasing the required torque for the attitude control. Hence in the following, a momentum management scheme will be included such that the total angular momentum of the wheels will become zero by applying some external torques to the spacecraft, when needed. It will be seen that this scheme will further reduce the occurrence of the singularity mentioned above.

The total momentum vector of the wheels is $\mathbf{A}\mathbf{h}_a$. If $\mathbf{A}\mathbf{h}_a = 0$ then $\mathbf{h}_a \in N(\mathbf{A})$; i.e.,

$$h^0_{a4} = -\sqrt{3}h^0_{ai},\ i = 1,2,3 \tag{35}$$

where the superscript 0 indicates the case when $\mathbf{h}_a \in N(\mathbf{A})$. If the momentum management is done when necessary (periodically once every one or two orbits, for example), the following equation is obtained from Eq. (35), which has opposite sign to Eq. (34), and hence the momentum management further eliminates the possibility of singularity,

$$h^0_{a4} = -\frac{\sqrt{3}}{3}\sum_{i=1}^{3} h^0_{ai} \tag{36}$$

Another way to see why proper momentum management eliminates the singularity problem is as follows. Equation $\mathbf{A}\mathbf{h}_a = 0$ implies that $\mathbf{h}_a \in N(\mathbf{A})$ and for a cluster with identical wheels (the typical case), using Eq. (5), also $\boldsymbol{\omega}_c \in N(\mathbf{A})$. Recall now that singularity occurs when $\boldsymbol{\omega}_c \in R(\mathbf{A}^T)$. But $N(\mathbf{A}) = R(\mathbf{A}^T)^{\perp}$ and after momentum management the wheel velocity vector is perpendicular to the singularity subspace $R(\mathbf{A}^T)$. The possibility of singularity has thus been reduced as much as possible. This does not, of course, include the case when $\boldsymbol{\omega}_c = 0$. The momentum management scheme above cannot be used in the zero wheel velocity case. However, since for safety margin the energy stored in the wheels always exceeds a certain level, the all-zero momentum wheel angular velocity can only happen during initial satellite deployment. This case is addressed in the next section.

The momentum management scheme in this paper is adopted from Ref. 32. The torque required for momentum management is

$$\mathbf{g}_e = -k(\mathbf{A}\mathbf{h}_a - \mathbf{A}\mathbf{h}_{an}) \tag{37}$$

where $\mathbf{h}_{an}$ denotes the nominal angular momentum vector of the wheels, and $k > 0$ is a feedback control gain. For the purpose of momentum unloading and singularity avoidance here we choose $\mathbf{A}\mathbf{h}_{an} = 0$.

Wheel Initialization

During initial satellite deployment, the wheels typically are in locked position and not spinning. It is important therefore to perform the initial spinning-up of the rotors, without affecting the attitude of the satellite. By the discussion in the previous sections, this can be achieved by using, for example, a constant torque $\mathbf{g}_a = \mathbf{g}_n \in N(\mathbf{A})$.

For the particular wheel configuration represented by the matrix $\mathbf{A}$ in Eq. (32), we can immediately calculate that

$$N(\mathbf{A}) = \text{span}\{\mathbf{u}\} = \text{span}\left\{\begin{bmatrix} 1 \\ 1 \\ 1 \\ -\sqrt{3} \end{bmatrix}\right\} \tag{38}$$

Therefore, if the wheels initially are not spinning, i.e., $\boldsymbol{\omega}_{ci} = 0$, $i = 1,2,3,4$, one can spin up the wheels to their assumed nominal speeds by applying a constant torque vector $\mathbf{g}_a = k_3\mathbf{u}$, where k_3 is a constant determined by the available torque of the wheels. Equation (5) shows that the wheels are spun up according to

$$\mathbf{I}_s\dot{\boldsymbol{\omega}}_c = k_3\mathbf{u} \tag{39}$$

Using this approach, after a period of t_{up} seconds the distribution of the angular velocities of the wheels is such that

$$\omega_{c4}(t_{up}) = \sum_{i=1}^{3} \omega_{ci}(t_{up})/\sqrt{3} \tag{40}$$

Numerical example

To demonstrate the aforementioned algorithm for the attitude and power tracking controller, the following numerical example has been performed. A near polar orbital satellite (orbital data chosen from the satellite IRIDIUM 25578) is considered in this simulation. The orbital elements are shown in Table 1. Here n is the orbital frequency,

Table 1 IRIDIUM 25578 orbital elements

n (rev/day)	14.57788549
M_0 (deg)	234.7460
ω (deg)	125.5766
Ω (deg)	132.8782
i (deg)	86.5318
e	0.00216220
Epoch	05/23/1999 00:16:12.24

M_0 is the mean anomaly at the epoch time, ω is the argument of perigee, Ω is the right ascension of the ascending node, i is the orbital inclination, and e is the eccentricity of the orbit. The satellite is assumed to have moment of inertia matrix

$$\mathbf{J} = \begin{bmatrix} 200 & 0 & 0 \\ 0 & 200 & 0 \\ 0 & 0 & 175 \end{bmatrix}\ \text{kg m}^2 \tag{41}$$

The normal power requirement of this satellite is 680 Watts. However, it is required to be able to provide instantaneous peak power of 4 kW for up to 5 minutes. Considering the 34 minutes eclipse time and assuming that the 4 kW peak power lasts 5 minutes, the momentum wheels should store at least 0.72 kWh energy. Taking into account a 100%

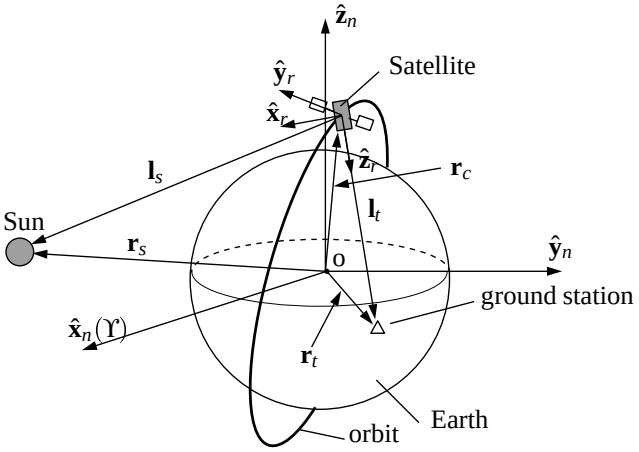

Fig. 2 The satellite mission illustration

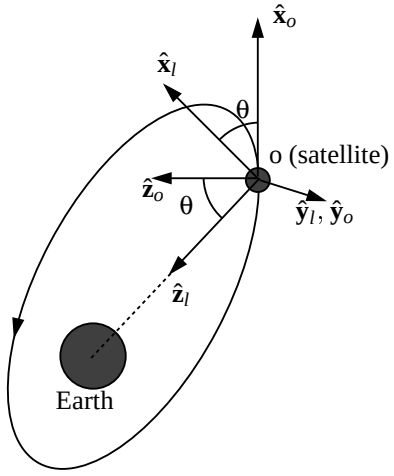

Fig. 3 The LVLH and orbital frames

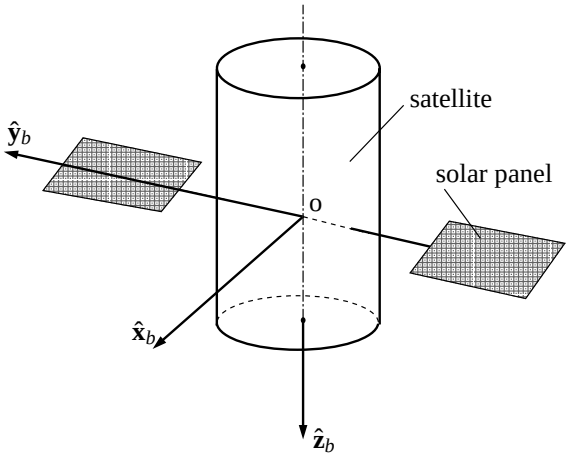

Fig. 4 The body frame

safety margin, the momentum wheels are required to store 1.5 kWh energy when they are fully charged. Suppose the nominal speed for the fourth wheel when the wheels are fully charged is 4000 rad/sec (38,197 rpm), and the speed for the other three 2309.4 rad/sec (22,053 rpm). These speeds render zero total angular momentum of the wheels. The energy and the wheel speed require that the wheels have moment of inertia of 0.338 kg m^2. Each momentum wheel is assumed to provide a maximum torque 1 Nm. In addition, the disturbance torque due to aerodynamics, solar pressure and other environmental factors is assumed to be[32]

$$\mathbf{g}_d = \begin{bmatrix} 4\times10^{-6}+2\times10^{-6}\sin(nt) \\ 6\times10^{-6}+3\times10^{-6}\sin(nt) \\ 3\times10^{-6}+3\times10^{-6}\sin(nt) \end{bmatrix} \text{N m} \qquad (42)$$

The satellite is required to perform sun and ground station tracking, namely, the symmetry axis should point to a ground station while the satellite is rotated by this axis such that the solar panel is perpendicular to the vector from the satellite to the sun. The ground station in this example is chosen to be Cape Canaveral (Longitude 80.467°W, Latitude 28.467°N). The sun and the ground station are assumed always available for the satellite. In the following, a brief description is given to illustrate the mission and the algorithm obtaining the reference attitude maneuver.

Mission definition

The scenario is shown in Fig. 2. The inertial frame is chosen to be the J2000 geocentric inertial coordinate system, denoted by the subscript n. The vectors $\mathbf{r}_s$, $\mathbf{r}_t$ and $\mathbf{r}_c$ denote the positions of the Sun, the Earth and the satellite, respectively, and the vector $\mathbf{l}_s$ and $\mathbf{l}_t$ denote the vectors from the satellite to the sun and the ground station. The following coordinate systems are used in the simulation besides the inertial frame, shown in Figs. 3 and 4. Hereafter, $\hat{(\cdot)}$ denotes a unit vector, and $\dot{(\cdot)}$ denotes the derivative taken in the inertial frame.

- Orbital frame, $o\hat{\mathbf{x}}_o\hat{\mathbf{y}}_o\hat{\mathbf{z}}_o$, with the $\hat{\mathbf{x}}_o$ axis pointing along the unit tangent of the orbital curve (the direction of the satellite velocity), the $\hat{\mathbf{y}}_o$ axis normal to the orbital plane, and the $\hat{\mathbf{z}}_o$ axis pointing along the unit normal to the orbit.

- Local Vertical Local Horizontal (LVLH) frame, $o\hat{\mathbf{x}}_l\hat{\mathbf{y}}_l\hat{\mathbf{z}}_l$, with the $\hat{\mathbf{z}}_l$ axis pointing towards the Earth center, and the $\hat{\mathbf{y}}_l$ axis the same as the $\hat{\mathbf{y}}_o$ axis. It is related to the orbital frame through a rotation at an angle θ about the $\hat{\mathbf{y}}_o$ axis (see Fig. 3)

- Body frame, $o\hat{\mathbf{x}}_b\hat{\mathbf{y}}_b\hat{\mathbf{z}}_b$, with the $\hat{\mathbf{z}}_b$ axis along the boresight axis, and the $\hat{\mathbf{y}}_b$ pointing along the solar panels.

The mission requires that at each moment along the orbit, the $\hat{\mathbf{z}}_b$ axis should track the ground station; i.e., $\hat{\mathbf{z}}_b$ tracks the unit vector along $\mathbf{l}_t$. In addition, the satellite should also track an attitude such that the $\hat{\mathbf{y}}_b$ axis is perpendicular to $\mathbf{l}_s$.

Computing the reference attitude profile

The satellite orbit is propagated by the orbit generator given in Ref. 33. From this, we know $\mathbf{r}_c$, $\dot{\mathbf{r}}_c$ and $\ddot{\mathbf{r}}_c$ in the

inertial frame at any time. The sun position ($\mathbf{r}_s$), velocity ($\dot{\mathbf{r}}_s$) and acceleration ($\ddot{\mathbf{r}}_s$) in the inertial frame are computed by the algorithm given in Ref. 34. The position ($\mathbf{r}_t$), velocity ($\dot{\mathbf{r}}_t$) and acceleration ($\ddot{\mathbf{r}}_t$) of the ground station in the inertial frame can be computed by converting the Universal Time (UT) into Greenwich Sidereal Time (GST).[33] From these, we know that

$$\mathbf{l}_s = \mathbf{r}_s - \mathbf{r}_c \tag{43a}$$
$$\dot{\mathbf{l}}_s = \dot{\mathbf{r}}_s - \dot{\mathbf{r}}_c \tag{43b}$$
$$\ddot{\mathbf{l}}_s = \ddot{\mathbf{r}}_s - \ddot{\mathbf{r}}_c \tag{43c}$$
$$\mathbf{l}_t = \mathbf{r}_t - \mathbf{r}_c \tag{43d}$$
$$\dot{\mathbf{l}}_t = \dot{\mathbf{r}}_t - \dot{\mathbf{r}}_c \tag{43e}$$
$$\ddot{\mathbf{l}}_t = \ddot{\mathbf{r}}_t - \ddot{\mathbf{r}}_c \tag{43f}$$

In the following, the attitude, angular velocity, and angular acceleration of the reference frame, which are the desired attitude, angular velocity, and angular acceleration for the body frame will be computed. The desired reference frame is denoted by $o\hat{\mathbf{x}}_r\hat{\mathbf{y}}_r\hat{\mathbf{z}}_r$ and is shown in Fig. 2.

The attitude reference

The rotation matrix $\mathbf{C}_N^L$ from the inertial frame to the LVLH frame can be readily computed by the orbital elements and $\mathbf{r}_c$ and $\dot{\mathbf{r}}_c$. Once the LVLH frame is known, we can write

$$\mathbf{l}_t = (\mathbf{l}_t \cdot \hat{\mathbf{x}}_l)\hat{\mathbf{x}}_l + (\mathbf{l}_t \cdot \hat{\mathbf{y}}_l)\hat{\mathbf{y}}_l + (\mathbf{l}_t \cdot \hat{\mathbf{z}}_l)\hat{\mathbf{z}}_l \tag{44}$$

so that

$$\hat{\mathbf{z}}_r = [(\mathbf{l}_t \cdot \hat{\mathbf{x}}_l)\hat{\mathbf{x}}_l + (\mathbf{l}_t \cdot \hat{\mathbf{y}}_l)\hat{\mathbf{y}}_l + (\mathbf{l}_t \cdot \hat{\mathbf{z}}_l)\hat{\mathbf{z}}_l]/\ell_t \tag{45}$$

where $\mathbf{l}_t = \ell_t \hat{\mathbf{l}}_t$. Since the $\hat{\mathbf{y}}_r$ axis is perpendicular to $\mathbf{l}_s$ and $\hat{\mathbf{z}}_r$, it can be computed by

$$\hat{\mathbf{y}}_r = \frac{\hat{\mathbf{z}}_r \times \hat{\mathbf{l}}_s}{|\hat{\mathbf{z}}_r \times \hat{\mathbf{l}}_s|} \tag{46}$$

and the $\hat{\mathbf{x}}_r$ axis is then given by

$$\hat{\mathbf{x}}_r = \hat{\mathbf{y}}_r \times \hat{\mathbf{z}}_r \tag{47}$$

From the unit vectors $\hat{\mathbf{x}}_r$, $\hat{\mathbf{y}}_r$, and $\hat{\mathbf{z}}_r$ we can compute $\mathbf{C}_N^R$, the rotation matrix from the inertial frame to the reference frame, and thus the attitude of the reference frame. The value of $\eta_s = \hat{\mathbf{l}}_s \cdot \hat{\mathbf{y}}_b$ will be used as a condition for sun tracking; i.e., $\eta_s = 0$ implies that the sun is being tracked. In addition, the value $\eta_t = |\hat{\mathbf{l}}_t \times \hat{\mathbf{z}}_b|$ will be used as a condition for ground station tracking; i.e., $\eta_t = 0$ implies that the ground station is being tracked.

The angular velocity and the angular acceleration reference

We proceed to compute the angular velocity of the reference frame with respect to the inertial frame expressed in the reference frame, $\boldsymbol{\omega}_R = [\omega_{rx},\ \omega_{ry},\ \omega_{rz}]^T$. The algorithm for computing ω_{rx} and ω_{ry} can be found in Ref. 35.

The derivative of the vector $\mathbf{l}_t$ in the inertial frame can be written in the desired reference frame as

$$\dot{\mathbf{l}}_t = (\dot{\mathbf{l}}_t \cdot \hat{\mathbf{x}}_r)\hat{\mathbf{x}}_r + (\dot{\mathbf{l}}_t \cdot \hat{\mathbf{y}}_r)\hat{\mathbf{y}}_r + (\dot{\mathbf{l}}_t \cdot \hat{\mathbf{z}}_r)\hat{\mathbf{z}}_r \tag{48}$$

Since $\dot{\mathbf{l}}_t$ can also be written as

$$\begin{aligned}\dot{\mathbf{l}}_t &= \frac{\mathrm{d}^R \mathbf{l}_t}{\mathrm{d}t} + \boldsymbol{\omega}_R \times \mathbf{l}_t \\ &= \frac{\mathrm{d}^R \mathbf{l}_t}{\mathrm{d}t} + \boldsymbol{\omega}_R \times (\ell_t \hat{\mathbf{z}}_r)\end{aligned} \tag{49}$$

where $\dfrac{\mathrm{d}^R \mathbf{l}_t}{\mathrm{d}t}$ is the derivative of $\mathbf{l}_t$ taken in the reference frame. Comparison of Eq. (48) and Eq. (49) yields

$$\omega_{rx} = -\frac{\dot{\mathbf{l}}_t \cdot \hat{\mathbf{y}}_r}{\ell_t} \tag{50}$$
$$\omega_{ry} = \frac{\dot{\mathbf{l}}_t \cdot \hat{\mathbf{x}}_r}{\ell_t} \tag{51}$$
$$\frac{\mathrm{d}^R \mathbf{l}_t}{\mathrm{d}t} = \dot{\mathbf{l}}_t \cdot \hat{\mathbf{z}}_r \tag{52}$$

Since $\hat{\mathbf{y}}_r \cdot \mathbf{l}_s = 0$, its time derivative

$$\dot{\hat{\mathbf{y}}}_r \cdot \mathbf{l}_s + \hat{\mathbf{y}}_r \cdot \dot{\mathbf{l}}_s = 0 \tag{53}$$

Expanding the derivative terms in the above equation, we end up with

$$\omega_{rz} = \frac{\omega_{rx}\mathbf{l}_s \cdot \hat{\mathbf{z}}_r + \hat{\mathbf{y}}_r \cdot \dot{\mathbf{l}}_s}{\mathbf{l}_s \cdot \hat{\mathbf{x}}_r} \tag{54}$$

The angular acceleration vector $\dot{\boldsymbol{\omega}}_R = (\dot{\omega}_{rx},\ \dot{\omega}_{ry},\ \dot{\omega}_{rz})^T$ can be obtained by taking the derivatives of ω_{rx}, ω_{ry} and ω_{rz}. By doing so, we get

$$\dot{\omega}_{rx} = -\frac{\ddot{\mathbf{l}}_t \cdot \hat{\mathbf{y}}_r + 2\omega_{rx}\dot{\ell}_t}{\ell_t} + \omega_{ry}\omega_{rz} \tag{55}$$
$$\dot{\omega}_{ry} = \frac{\ddot{\mathbf{l}}_t \cdot \hat{\mathbf{x}}_r - 2\omega_{ry}\dot{\ell}_t}{\ell_t} - \omega_{rx}\omega_{rz} \tag{56}$$
$$\dot{\omega}_{rz} = \frac{\dot{M}N - M\dot{N}}{N^2} \tag{57}$$

where

$$M = \omega_{rx}\mathbf{l}_s \cdot \hat{\mathbf{z}}_r + \hat{\mathbf{y}}_r \cdot \dot{\mathbf{l}}_s \tag{58}$$
$$N = \mathbf{l}_s \cdot \hat{\mathbf{x}}_r \tag{59}$$
$$\dot{M} = \dot{\omega}_{rx}\mathbf{l}_s \cdot \hat{\mathbf{z}}_r + \omega_{rx}\dot{\mathbf{l}}_s \cdot \hat{\mathbf{z}}_r + \omega_{rx}\mathbf{l}_s \cdot (\boldsymbol{\omega}_R \times \hat{\mathbf{z}}_r) + \boldsymbol{\omega}_R \times \hat{\mathbf{y}}_r \cdot \dot{\mathbf{l}}_s + \hat{\mathbf{y}}_r \cdot \ddot{\mathbf{l}}_s \tag{60}$$
$$\dot{N} = \dot{\mathbf{l}}_s \cdot \hat{\mathbf{x}}_r + \mathbf{l}_s \cdot (\boldsymbol{\omega}_R \times \hat{\mathbf{x}}_r) \tag{61}$$

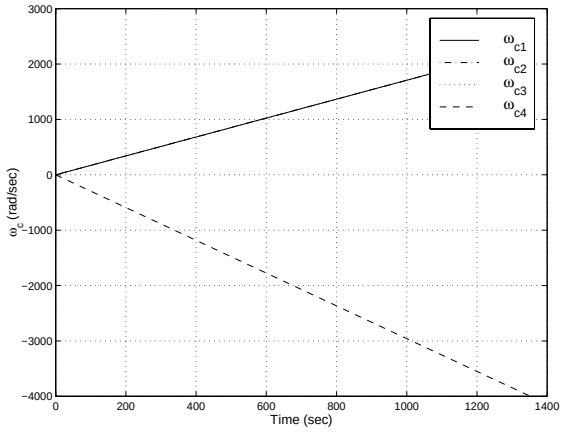

Fig. 5 The angular velocity of the momentum wheels during initialization (spin-up).

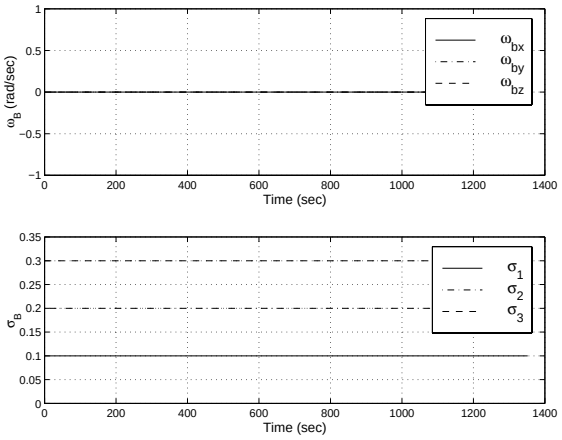

Fig. 6 Attitude and body angular velocity during initialization (spin-up).

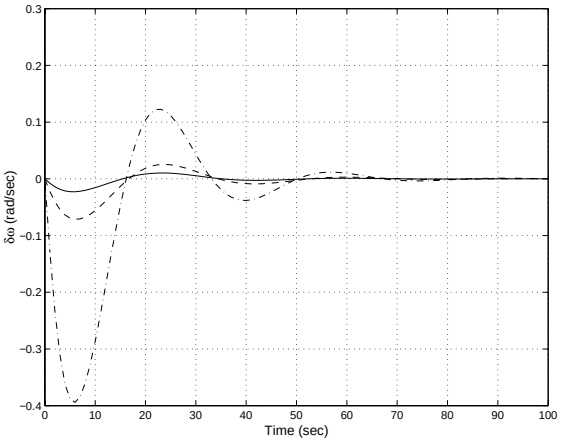

Fig. 7 The error in angular velocity of the satellite during target acquisition.

Simulation results

With the reference satellite attitude profile computed in the previous section, we can apply the attitude and power tracking controller. Three simulations are conducted in a sequence. First, the momentum wheels are initialized by spinning up the wheels without affecting the attitude, see Eq. (39); second, a target acquisition maneuver is performed where the satellite is maneuvered from the LVLH frame to the required sun and ground station tracking attitude; finally, energy storage function is switched on and the momentum wheels are used to keep tracking the sun and the ground station. In the simulation, quaternions are used to describe the attitude from the inertial frame to the body and reference frame due to the large angle orbital maneuver, and MRPs are used to describe the difference between the body and the reference frame. The results are presented in the following three subsections.

Initialization of momentum wheels

This simulation demonstrates the initialization of the wheels from a zero-spin situation to their nominal values of $\omega_{ci} = 2309.4$ (rad/sec) for $i = 1,2,3$ and $\omega_{c4} = -4000$ (rad/sec). Notice that after a period of $t_{up} = 1352$ sec the wheel speeds satisfy the condition in Eq. (40). During the spin-up a constant torque is applied, equal to $\mathbf{g}_a = [1/\sqrt{3}\ 1/\sqrt{3}\ 1/\sqrt{3}\ -1]^T$ (Nm). Here the satellite is initially in the rest position with attitude which is given in terms of MRPs as $(0.1, 0.2, 0.3)^T$. The wheel angular velocity during spin-up is shown in Fig. 5. The corresponding attitude and angular velocity for the body are shown in Fig. 6. From this figure it is seen that the wheel speed initialization does not affect the satellite attitude, as expected.

Target acquisition

After the momentum wheel speeds are initialized, the satellite attitude will be controlled, such that the sun and the ground station are tracked. The simulation starts with the satellite body frame aligned with the LVLH frame. Because this initial target acquisition maneuver is usually a fast, large angle (slew) maneuver, and the momentum wheels are of fairly low control authority (1 Nm in this example), we use external thrusters to issue the required torque; i.e., in Eq. (17), we choose

$$\mathbf{A}\mathbf{g}_a = 0 \tag{62}$$

$$\begin{aligned}\mathbf{g}_t = &-\mathbf{h}_B^{\times}\mathbf{J}^{-1}(\mathbf{h}_B - \mathbf{A}\mathbf{h}_a) - \mathbf{g}_g + \mathbf{J}\boldsymbol{\omega}_B^{\times}\delta\boldsymbol{\omega} \\ &+ \mathbf{J}\mathbf{C}_R^B(\delta\boldsymbol{\sigma})\mathbf{J}^{-1}\mathbf{h}_R^{\times}\mathbf{J}^{-1}\mathbf{h}_R + \mathbf{J}\mathbf{C}_R^B(\delta\boldsymbol{\sigma})\mathbf{J}^{-1}\mathbf{g}_R \\ &- k_1\delta\boldsymbol{\omega} - k_2\delta\boldsymbol{\sigma}\end{aligned} \tag{63}$$

The controller gains are chosen as $k_1 = 24$ and $k_2 = 27$. Figure 7 shows the angular velocity tracking error of the satellite, and Fig. 8 shows the quaternions of the body frame and the reference frame. It is seen that after about 70 sec the satellite attitude tracks the reference. In Fig. 9 it is shown that the sun tracking condition value η_s goes to zero after about 90 seconds. In Fig. 10 it is shown that the ground station tracking condition value η_t goes to zero also after about 90 seconds. Figure 11 shows the torque required to perform the target acquisition maneuver.

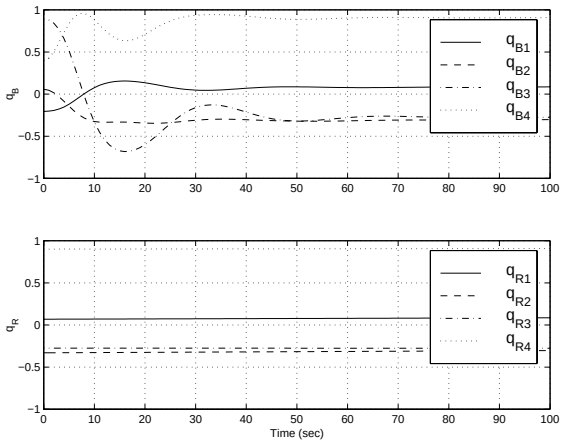

Fig. 8 Quaternions during target acquisition ($\mathbf{q}_B \to \mathbf{q}_R$).

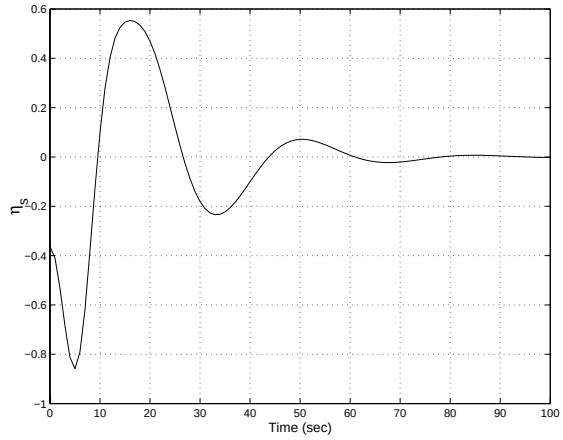

Fig. 9 The sun tracking condition during target acquisition ($\eta_s = \hat{\mathbf{l}}_s \cdot \hat{\mathbf{y}}_b$).

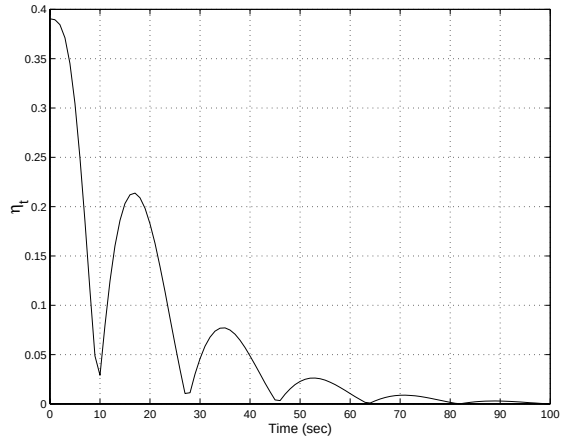

Fig. 10 The ground station tracking condition during target acquisition ($\eta_t = |\hat{\mathbf{l}}_t \times \hat{\mathbf{z}}_b|$).

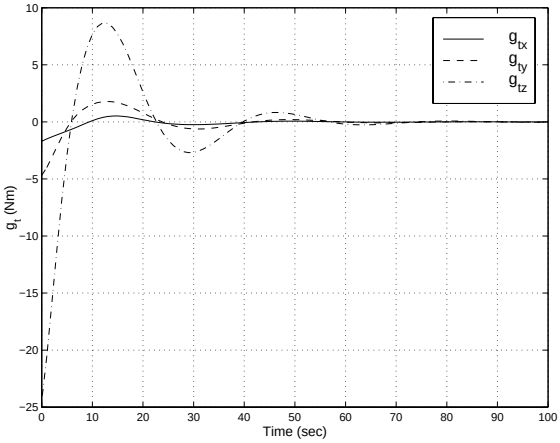

Fig. 11 The required thruster torque for the target acquisition ($\mathbf{g}_a = 0$).

Continuous tracking

After the satellite tracks the sun and the ground station, the momentum wheels attitude control and energy storage are switched on, so that the satellite will keep tracking the sun and the ground station. In this case, the momentum wheels will provide both the target tracking torques and the energy storage torques. The thrusters will only be used to issue the necessary momentum management torque; i.e., in Eq. (17), we choose

$$\mathbf{g}_t = -k(\mathbf{A}\mathbf{h}_a - \mathbf{A}\mathbf{h}_{an}) \quad \text{every two orbits} \tag{64}$$

and

$$\begin{aligned}\mathbf{A}\mathbf{g}_a =& \mathbf{h}_B^{\times}\mathbf{J}^{-1}(\mathbf{h}_B - \mathbf{A}\mathbf{h}_a) + \mathbf{g}_t + \mathbf{g}_g - \mathbf{J}\boldsymbol{\omega}_B^{\times}\delta\boldsymbol{\omega} \\ & - \mathbf{J}\mathbf{C}_R^B(\delta\boldsymbol{\sigma})\mathbf{J}^{-1}\mathbf{h}_R^{\times}\mathbf{J}^{-1}\mathbf{h}_R - \mathbf{J}\mathbf{C}_R^B(\delta\boldsymbol{\sigma})\mathbf{J}^{-1}\mathbf{g}_R \\ & + k_1\delta\boldsymbol{\omega} + k_2\delta\boldsymbol{\sigma}\end{aligned} \tag{65}$$

The simulation orbit starts from 02/23/99 07:59:32.28 and lasts for 25,000 seconds (about 4 orbits). The controller gains are chosen as $k_1 = 24$, $k_2 = 27$, and $k = 0.005$. During the eclipse, the wheels provide 680 Watt power and 4 kW power for 5 minutes. During sunlight, the wheels are charged with a power level of 1 kW until the total energy stored in the wheels reaches 1.5 kWh. After the wheels are charged, the momentum management is switched on every two orbits. Figure 12 shows the satellite angular velocity and the reference angular velocity. Figure 13 shows the comparison between the quaternions of the body frame and those of the reference frame. These two figures show that the body frame keeps tracking the reference attitude profile closely. Figures 14 and 15 show that the sun and ground station tracking conditions are being satisfied. Figure 16 shows the power profile with the sunlight and eclipse indication, where sunlight is indicated by 1 and eclipse is indicated by -1. The corresponding torque applied by the momentum wheels is shown in Fig. 17, along with the total angular momentum of the wheels. It is seen that every two orbits (at about 0.6×10^4 and 1.8×10^4 seconds in Fig. 17) the total angular momentum of the wheels, $\mathbf{A}\mathbf{h}_a$ goes

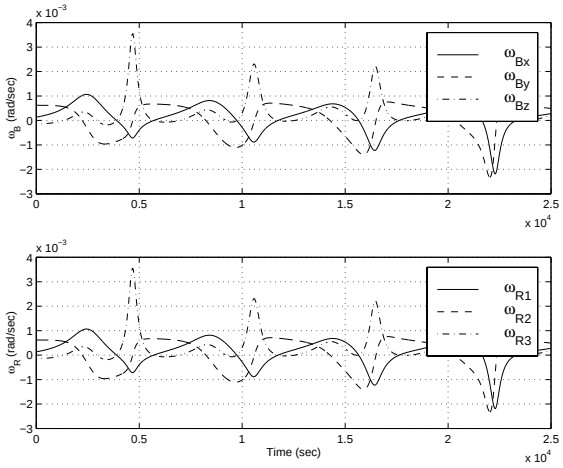

Fig. 12 The angular velocity of the satellite during tracking ($\boldsymbol{\omega}_B \to \boldsymbol{\omega}_R$, $\mathbf{g}_t = 0$).

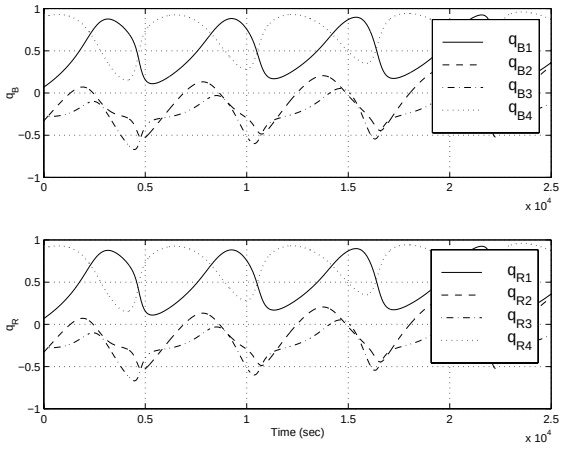

Fig. 13 Quaternions during tracking ($\mathbf{q}_B \to \mathbf{q}_R$, $\mathbf{g}_t = 0$).

to zero due to proper momentum management. Figure 18 shows the momentum wheel angular velocities. The momentum management torque is shown in Fig. 19.

Conclusion

In this paper, we develop an algorithm for controlling the spacecraft attitude while simultaneously tracking a desired power profile, using a cluster of more than three non-coplanar momentum wheels. The torque is decomposed into two perpendicular spaces. One is the null space of the matrix whose columns are the unit vectors along the axes of each momentum wheel. The torque in this space is used to track the required power level of the wheels, while the torque in the space perpendicular to the null space of the matrix is used to control the attitude of the satellite.

The torque decomposition is based on solving a set of linear equations. Singularities may occur in case when the coefficient matrix does not have full row rank. In this case, no arbitrary power profile can be tracked. A momentum management scheme is considered to null the total angular momentum of the momentum wheels in order to minimize

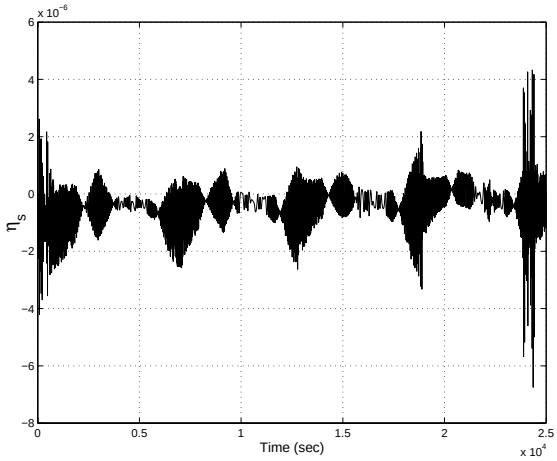

Fig. 14 The sun tracking condition during tracking ($\eta_s = \mathbf{l}_s \cdot \hat{\mathbf{y}}_b$).

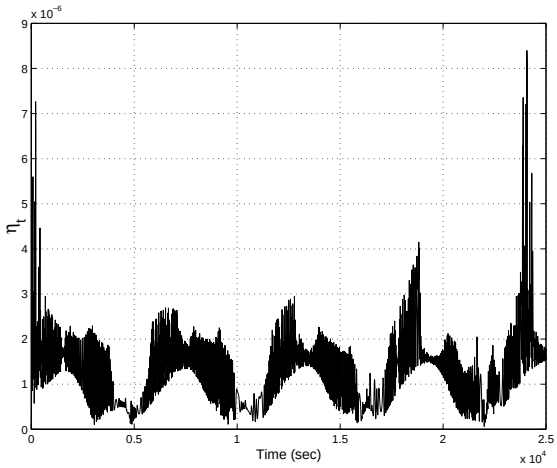

Fig. 15 The ground station tracking condition during tracking ($\eta_t = |\mathbf{l}_t \times \hat{\mathbf{z}}_b$).

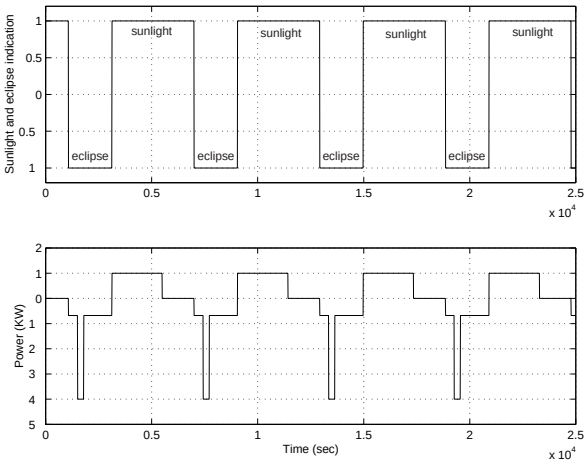

Fig. 16 Sunlight/eclipse indication and power profile.

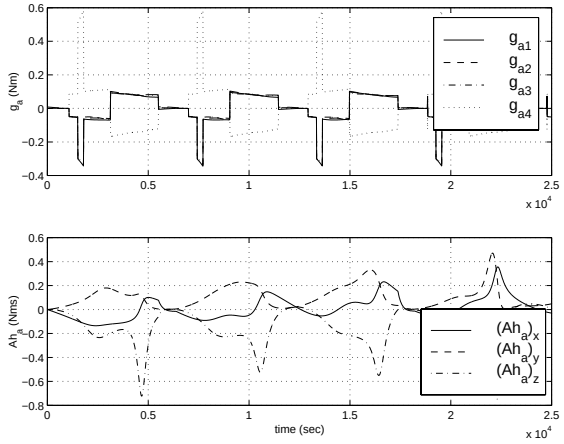

Fig. 17 The axial torques and the total angular momentum of the momentum wheels.

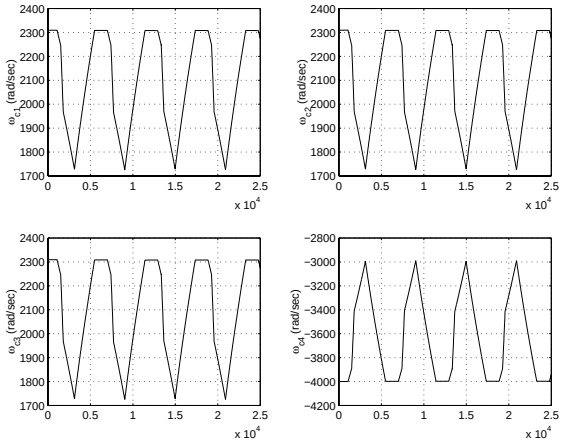

Fig. 18 The angular velocities of the momentum wheels .

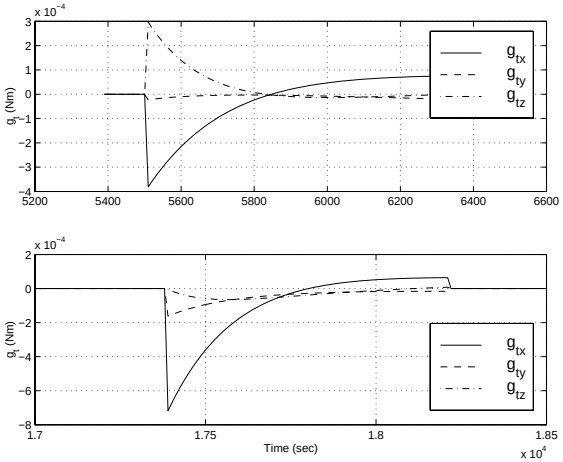

Fig. 19 The momentum management torque (upper figure for the 1st orbit, and lower figure for the 3rd orbit).

the gyroscopic effect and also prevent the occurrence of singularities.

A numerical example based on a realistic scenario of an IRIDIUM-type satellite demonstrates the efficacy of the proposed algorithm.

References

[1]Wertz, J. and Larson, W., Eds., *Space Mission Analysis and Design*. Boston, Kluwer Academic Publishers, 1991.

[2]Roes, J. B., "An Electro-Mechanical Energy Storage System for Space Application," in *Progress in Astronautics and Rocketry*, Vol. 3, (New York), pp. 613–622, Academic Press, 1961.

[3]Adams, L. R., "Application of Isotensoid Flywheels to Spacecraft Energy and Angular Momentum Storage," tech. rep., Technical Report NASA CR-1971, Astro Research Corporation, Santa Barbara, California, 1972.

[4]Anderson, W. W. and Keckler, C. R., "An Integrated Power/Attitude Control System (IPACS) for Space Application," in *Proceedings of the 5th IFAC Symposium on Automatic Control in Space*, 1973.

[5]Cormack III, A., "Three Axis Flywheel Energy and Control Sytems," tech. rep., Technical Report TN-73-G&C-8, North American Rockwell Corporation, 1973.

[6]Keckler, C. R. and Jacobs, K. L., "A Spacecraft Integrated Power/Attitude Control System," in *9th Intersociety Energy Conversion Engineering Conference*, 1974.

[7]Will, R. W., Keckler, C. R., and Jacobs, K. L., "Description and Simulation of an Integrated Power and Attitude Control System Concept for Space-Vehicle Application," tech. rep., Technical Report TN D-7459, NASA, 1974.

[8]Notti, J. E., Cormack III, A., Schmill, W. C., and Klein, W. J., "Integrated Power/Attitude Control System (IPACS) Study: Volume II–Conceptual Designs," tech. rep., Technical Report NASA CR-2384, Rockwell International Space Division, Downey, California, 1974.

[9]Rodriguez, G. E., Studer, P. A., and Baer, D. A., "Assessment of Flywheel Energy Storage for Spacecraft Power Systems," tech. rep., Technical Report NASA TM 85061, NASA Goddard Flight Center, Greenbelt, Maryland, 1983.

[10]Gross, S., "Study of Flwheel Energy Storage for Space Stations," tech. rep., Technical Report NASA CR-171780, Boeing Aerospace Co., Seattle, Washington, 1984.

[11]Keckler, C. R., Rodriguez, G. E., and Groom, N. J., Eds., *Integrated Flywheel Technology 1983*. Number NASA CP-2290, 1983.

[12]Anand, D., Kirk, J. A., and Frommer, D. A., "Design Considerations for Magnetically Suspended Flywheel systems," in *Proceedings of the 20th Intersociety Energy Conversion Engineering Conference*, Vol. 2, pp. 449–453, 1985.

[13]Anand, D., Kirk, J. A., Amood, R. B., Studer, P. A., and Rodriguez, G. E., "System Considerations for Magnetically Suspended Flywheel systems," in *Proceedings of the 21st Intersociety Energy Conversion Engineering Conference*, Vol. 3, pp. 1829–1833, 1986.

[14]Downer, J., Eisenhaure, D., Hockney, R., Johnson, B., and O'Dea, S., "Magnetic Suspension Design Options for Satellite Attitude Control and Energy Storage," in *Proceedings of the 20th Intersociety Energy Conversion Engineering Conference*, Vol. 2, pp. 424–430, 1985.

[15]Flatley, T., "Tetrahedron Array of Reaction Wheels for Attitude Control and Energy Storage," *Proceedings of the 20th Intersociety Energy Conversion Engineering Conference*, Vol. 2, 1985, pp. 2353–2360.

[16]O'Dea, S., Burdick, P., Downer, J., Eisenhaure, D., and Larkin, L., "Design and Development of a High Efficiency Effector for the Control of Attitude and Power in Space Systems," in *Proceedings of the 20th Intersociety Energy Conversion Engineering Conference*, Vol. 2, pp. 353–360, 1985.

[17]Oglevie, R. E. and Eisenhaure, D. B., "Advanced Integrated Power and Attitude Control System (IPACS) Technology," tech. rep., Tecnical Report NASA CR 3912, November, 1985.

[18]Oglevie, R. E. and Eisenhaure, D. B., "Integated Power and Attitude control System (IPACS) Technology," in *Proceedings of the 21st Intersociety energy Conversion Engineering Conference*, Vol. 3, pp. 1834–1837, 1986.

[19]Olmsted, D. R., "Feasibility of Flywheel Energy Storage in Spacecraft Applications," in *Proceedings of the 20th Intersociety energy Conversion Engineering Conference*, Vol. 2, pp. 444–448, 1985.

[20]Studer, P. and Rodriguez, E., "High Speed Reaction Wheels for Satellite Attitude Control and Energy Storage," in *Proceedings of the 20th Intersociety energy Conversion Engineering Conference*, Vol. 2, pp. 349–352, 1985.

[21]Van Tassel, K. E. and Simon, W. E., "Inertial Energy Storage for Advanced Space Station Application," in *Proceedings of the 20th Intersociety energy Conversion Engineering Conference*, Vol. 2, pp. 337–342, 1985.

[22]Olszewski, M., "Development of Regenerable Energy Storage for Space Multi-megawatt Applications," in *Proceedings of the 21st Intersociety energy Conversion Engineering Conference*, Vol. 3, pp. 1838–1841, 1986.

[23]Olszewski, M. and O'Kain, D. U., "Advances in Flywheel Technology for Space Power Applications," in *Proceedings of the 21st Intersociety energy Conversion Engineering Conference*, Vol. 3, pp. 1823–1828, 1986.

[24]Santo, G. E., Gill, S. P., Kotas, J. F., and Paschall, R., "Feasibility of Flywheel Energy Storage Systems for Applications in Future Space Missions–Final Contractor Report," tech. rep., Technical Report NASA-CR-195422, Rockwell International Corporation, January, 1995.

[25]Tsiotras, P., "Stabilization and Optimality Results for the Attitude Control Problem," *Journal of Guidance, Control, and Dynamics*, Vol. 19, No. 4, 1996, pp. 772–777.

[26]Schaub, H., Robinett, R., and Junkins, J., "Stereographic Orientation Parameters for Attitude Dynamics: A Generalization of the Rodrigues Parameters," *Journal of the Astronautical Sciences*, Vol. 44, No. 1, 1996, pp. 1–19.

[27]Tsiotras, P., Junkins, J., and H., S., "Higher Order Cayley-Transforms with Applications to Attitude Representations," *Journal of Guidance, Control, and Dynamics*, Vol. 20, No. 3, 1997, pp. 528–534.

[28]Hall, C., Tsiotras, P., and Shen, H., "Tracking Rigid Body Motion Using Thrusters and Reaction Wheels," in *Proceedings of Astrodyamics Specialists Conference*, (Boston, MA.), August 10-12, 1998. AIAA paper 984471.

[29]Hughes, P., *Spacecraft Attitude Dynamics*. New York, John Wiley & Sons, 1986.

[30]Khalil, H., *Nonlinear Systems*. Upper Saddle River, NJ 07458, Prentice hall, 2nd ed., 1996.

[31]Hall, C., "High-speed Flywheels for Integrated Energy Storage and Attitude Control," *American Control Conference*, Vol. 3, 1997, pp. 1894–1898.

[32]Sidi, M., *Spacecraft Dynamics and Control, A Practical Engineering Approach*. New York, Cambridge University Press, 1997.

[33]Wertz, J., Ed., *Spacecraft Attitude Determination and Control*. Boston, Reidel, 1997.

[34]Meeus, J., *Astronomical Algorithms*. Richmond, Virginia, Willmann-Bell, 1991.

[35]Hablani, H., "Design of a Payload Pointing Control system for Tracking Moving Objects," *Journal of Guidance, Control, and Dynamics*, Vol. 12, No. 3, 1989, pp. 365–374.